

A Sensor Fusion Method on Local Homing Robot Navigation Using Omnidirectional Sensor-Based Model and Fuzzy Arithmetic

전방향 센서 기반의 모델과 퍼지 연산을 이용한 국부 유도 로봇 항법용 센서 융합 방법

Seok Won Bang and Myung Jin Chung
(방 석 원, 정 명 진)

요 약 : 본 논문에서는 초음파 센서와 시각 센서에서 얻은 전방향 센서 데이터를 이용하여 실내 이동 로봇용 국부 유도 항법을 위한 새로운 환경 모델링 방법을 제안한다. 그리고 이 두 종류의 센서 데이터에 포함된 불확실성을 주관적 지식과 퍼지 연산법을 사용하여 정량적으로 다룰 수 있는 센서 융합법을 제안한다. 이 방법을 사용하여, 로봇의 현재 위치와 목표 위치간의 기하학적 관계를 더욱 정확하게 얻을 수 있다. 실험 결과를 통하여 제안된 모델링과 센서 융합법이 실내 이동 로봇 항법에 효과적임을 보였다.

Keywords: omnidirectional sensor-based modeling, local homing navigation, sensor fusion, fuzzy arithmetic

I. Introduction

The main tasks of the indoor mobile robot navigation are to find out the position of robot in the global map and to know the geometric relations between the current location and the target location. The appropriate modeling of robot environment, the acquisition of sensor data through a variety of sensors, and the inference of the geometric relations using sensor data fusion are essential to accomplish given tasks successfully. The model based navigation which adopts a stereo vision or a range finder for mobile robot navigation needs a lot of memory space and processing time. It has proved to be a complex and time-consuming task, even in a task domain where the robot is given a 3D model of its environment[1][2]. In general, it is difficult to extract sufficient 3D information through sensors, so the model-based method is not appropriate for the indoor mobile robot navigation. On the other hand, the image-based homing is more practical and efficient since it need not build a 3D model of the environment[3][4]. However, in this approach, it is quite difficult to compute the exact direction or distance to the target location and this scheme is applicable only to the spatially limited space. Jiawei Hong et al.[5] proposed an image-based local homing algorithm to navigate between neighboring target locations. This approach used an imaging system to project a full 360° view of the world into a single image and then condensed this view into a compact and one-dimensional location signature. Hence, it may have less computation time and memory size than the others. But this method has the following disadvantages: First, it is impossible to obtain the unique solution of the spatial relation since this method uses only the one-dimensional data. Second, the robot should move many times to reach the target

location because the obtained relation is imprecise. Finally, the rules cannot properly manipulate the uncertainty of environment model.

Recently, various sensors are used to improve the intelligence and to obtain more accurate spatial relation for the robot[6][7]. Since more uncertainties generate as the number of sensors increases, a sensor fusion method is required to deal with uncertainties. The probabilistic approach has dominated much of the work on the representation and manipulation of uncertainties[8]. However, it is a difficult task to obtain the probability density functions(p.d.f.) for a variety of environment[1][9]. Even though we know the p.d.f.s, the calculation itself is too complicate. Moreover, the subjective knowledge of the expert cannot be represented[10].

In this paper, we propose a new environment modeling method for local homing of the indoor mobile robot using the omnidirectional sensor data obtained by an ultrasonic sensor and a vision sensor. We also develop a sensor fusion method that can deal with the uncertain sensor data. The proposed method uses fuzzy numbers in order to represent the subjective knowledge and manipulates the operation of uncertain quantities using fuzzy arithmetic. It has constraints such that the orientation of the robot relative to the ground plane does not change and the ground remains level. The experiment results show the effectiveness of the proposed model and method.

II. Omnidirectional Sensor-Based Local Homing Method

In robotics, homing is to find a fixed target location which is known to the robot. The robot is capable of finding its way only to these fixed target locations but not to any arbitrary locations in its environment. Especially in local homing, the target location is close enough to the current location of the robot[5]. If the robot has the environment models of many target

접수일자 : 1995. 6. 15.

1차 수정 : 1995. 8. 30., 2차 수정 : 1995. 9. 12.

방석원 : 한국과학기술원 전기 및 전자공학과

정명진 : 한국과학기술원 전기 및 전자공학과

locations in advance, it can reach the final target location via the intermediate targets. Therefore, the navigation task is divided into several simple local tasks that require the ability to reach the nearest target location. Namely, the goal of local homing is to reach an intermediate target location from the robot's current location. For this purpose, the data of environment model should be compact and should be easily obtained. To construct this model, we make use of the omnidirectional sensor data obtained from a scanner.

2.1 Geometric Relation

The whole task can be described as the iteration of local homing. In each local task, it is assumed that the orientation of the robot relative to the ground does not change and that the ground remains same level. Fig. 1 shows the geometric relation of the current location, the target location, and the feature point. The distance l and the orientation α to the current location from the target location can be uniquely determined by the following equation.

$$l = \sqrt{r_t^2 + r_c^2 - 2 r_t r_c \cos(\theta_t - \theta_c)} \quad (2.1)$$

$$\alpha = \tan^{-1} \left(\frac{r_t \sin(\theta_t) - r_c \sin(\theta_c)}{r_t \cos(\theta_t) - r_c \cos(\theta_c)} \right)$$

where r_t, r_c are the distances to the feature point from the target location and the current location respectively, and θ_t, θ_c are the orientations of feature point with respect to the target location and the current location respectively.

Namely, if we know the values ($r_t, r_c, \theta_t, \theta_c$), we can get the geometric relation between the two locations.

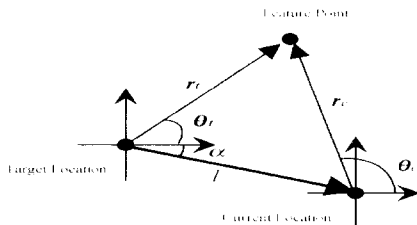


Fig. 1. Geometric relation of the current location, the target location, and the feature point.

2.2 Obtaining and Storage of Sensor Data

A CCD camera and an ultrasonic sensor are widely used for the mobile robot navigation. The sensor data is already obtained by means of the scanner which can rotate with resolution of 0.1 degree. Fig. 2 shows the structure of the scanner.

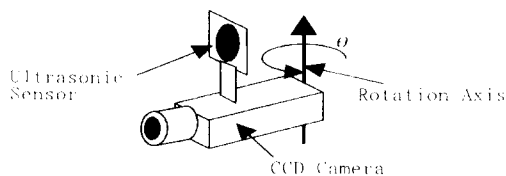
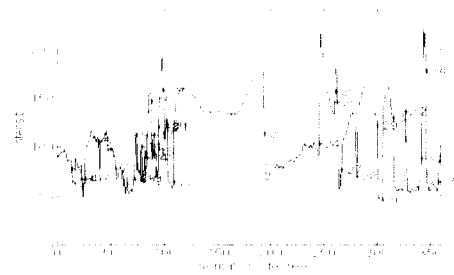


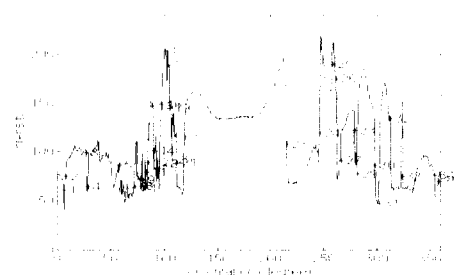
Fig. 2. Structure of the scanner.

The focal axis of camera is perpendicular to the rotation axis which is normal to the ground. The horizontal plane is defined as the plane surface that is parallel to the ground and that includes the focal axis. Assuming that the orientation of the robot relative to the

ground plane does not change and the ground remains level, the feature points that are seen in the horizontal plane at one location will be in the horizon plane at another location. We can extract one dimensional intensity data, $I(\theta)$ and range data, $R(\theta)$ by omnidirectional sampling. Fig. 3 shows the examples of the intensity data measured at the current location and the target location. And Fig. 4 shows examples of the range data measured at the same locations of Fig. 3.

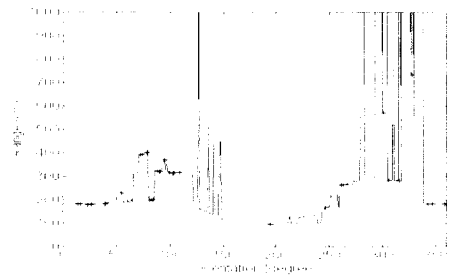


(a) $I_c(\theta)$

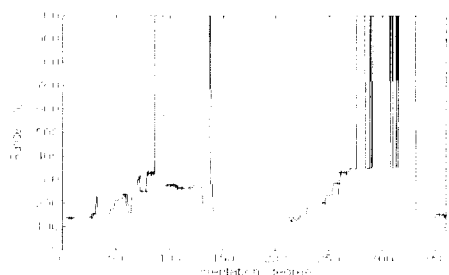


(b) $I_t(\theta)$

Fig. 3. Examples of the intensity data from CCD camera. (a) Intensity data measured at the current location, (b) Intensity data measured at the target location.



(a) $R_c(\theta)$



(b) $R_t(\theta)$

Fig. 4. Examples of the range data from ultrasonic sensor. (a) Range data measured at the current location, (b) Range data measured at the target location.

2.3 Modeling the Robot Environment

For a sensor-based local homing navigation, a modeling of the robot environment is essential to accomplish a given task successfully. In this paper, we propose a new environment model for local homing of the robot using the omnidirectional sensor data of an ultrasonic sensor and a vision sensor. In general, since it is difficult to elicit sufficient 3D information through sensors because of the uncertainties, 3D modeling of robot environment is not appropriate for the indoor mobile robot navigation. Therefore, we model the environment with a set of landmarks extracted from omnidirectional sensor data. Since the image of indoor environment is mainly composed of vertical and horizontal line, we can use the vertical edges as prominent landmark. A landmark, as called a feature point, is easily obtained from the intensity data, $I(\theta)$ through the following steps:

- Step 1. Low-pass Filtering: We reduce the high frequency noise.
- Step 2. Scaling: To reduce the effect of luminescence variation, we normalize the intensity data set so that it has zero mean and unit standard deviation.
- Step 3. Edge Detection: Using the first order derivative edge detection, we find edge points.[13]
- Step 4. Constructing Feature Set, $F = \{F_1, \dots, F_i, \dots, F_n\}$: F_i is the feature point at the i th edge point obtained by Step 3 and n is the number of feature.

F_{ci} and F_{tj} are the i th feature point in the current location and the j th feature point in the target location respectively. F_{ci} and F_{tj} have the following attributes:

- $\hat{\theta}_i$: the measured orientation of i th feature.
- \hat{r}_i : the measured range of i th feature.
- I_{r_i}, I_{l_i} : the average value of intensities between $\hat{\theta}_{i-1}$ and $\hat{\theta}_i$, $\hat{\theta}_i$ and $\hat{\theta}_{i+1}$ respectively.
- g_i : $\frac{dI}{d\theta}|_{\theta=\hat{\theta}_i}$, the intensity gradient of i th feature.
- w_{c_i} : the angular width of orientation having the same range at the i th feature.
- w_{m_i} : the angular distance to the i th feature orientation from the center of w_{c_i} .
- w_{sr_i}, w_{sl_i} : the angular differences of $\hat{\theta}_{i-1}$ and $\hat{\theta}_i$, $\hat{\theta}_i$ and $\hat{\theta}_{i+1}$ respectively.

Fig. 5 shows the relation of the attributes and the feature points

We can represent the uncertainties of $\hat{\theta}_i, \hat{r}_i$ with the attributes. The numbers denoted in Fig. 3 are the i, j values of feature points. And the parts denoted as + in Fig. 3 and in Fig. 4 are the feature points.

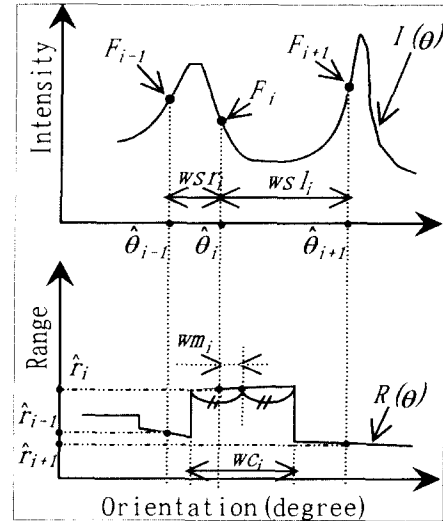


Fig. 5. Relation of attributes and feature points.

2.4 Matching of Feature Points

The goal of the matching step is to find a set of correspondences between the feature points in the omnidirectional sensor data obtained at the current location and the target location. We can match F_{ci} in the current location to F_{tj} in the target location as following steps:

- Step 1. Find a set of F_{tj} satisfying $|\hat{\theta}_{ci} - \hat{\theta}_{tj}| \leq 30^\circ, \hat{r}_t < 10m, i : \text{fixed},$ and $j : 1, \dots, n$. Note that n is the number of feature points in the target location. Since the target location is close to the current location and the maximum sensing range of the ultrasonic sensor is 10m, we restrict the comparison feature points.
- Step 2. Find a set of F_{tj} in the set obtained from step 1 satisfying $|g_{ci} - g_{tj}| < \delta$ where δ is chosen properly.
- Step 3. Find a set of F_{tj} in the set obtained from step 2 satisfying $|r_{ci} - r_{tj}| + |I_{r_i} - I_{r_j}| < \epsilon$ where ϵ is chosen properly.
- Step 4. Select the F_{tj} which has the minimum value of $|\hat{\theta}_{ci} - \hat{\theta}_{tj}|$ if the number of element in the set obtained from step 3 is not one.
- Step 5. If $\hat{r}_{ci} < 10m$, we match F_{ci} to F_{tj} obtained from step 4.

In the case of Fig. 3 and Fig. 4, the finally matched feature points, F_{ci} and F_{tj} are $(F_{c6}, F_{t4}), (F_{c3}, F_{t8}), (F_{c23}, F_{t23}),$ and (F_{c25}, F_{t25}) .

III. Fusion of Sensor Data

The main task of the sensor-based local homing is to find out the geometric relations, distance l and orientation α between the current location and the target location. If the set of $\{r_c, r_t, \theta_c, \theta_t\}$ is exact and unique, we can uniquely determine the exact l and α by (2.1). However, we cannot know the exact values

because the sensory measurements have uncertainty. Moreover, the number of successfully matched (i, j) pairs may be more than one. Therefore, all the variables in (2.1) must be replaced with their measured values as like (3.1).

$$l_{ij} = \sqrt{r_{ij}^2 + r_{ci}^2 - 2r_{ij}r_{ci}\cos(\theta_{ij} - \theta_{ci})}$$

$$\alpha_{ij} = \tan^{-1}\left(\frac{r_{ij}\sin(\theta_{ij}) - r_{ci}\sin(\theta_{ci})}{r_{ij}\cos(\theta_{ij}) - r_{ci}\cos(\theta_{ci})}\right) \quad (3.1)$$

where r_{ij} , r_{ci} , θ_{ij} , and θ_{ci} are the measured values of r_{ij} , r_{ci} , θ_{ij} , and θ_{ci} respectively.

To acquire more precise geometric relation, we must take account of the uncertainties in the sensory measurement. The probabilistic approach has dominated much of the work on the representation and manipulation of uncertainties. However, it is a difficult task to obtain the probability density function(p.d.f.) for a variety of environment. Though we know the p.d.f., the calculation is complicated. But we can describe the uncertainties qualitatively by use of possibility which enables us to represent the subjective knowledge of the expert. By introducing fuzzy number, we can deal with the uncertainties depending on the expert's preference or experience. Therefore, (3.1) can be rewritten by (3.2) as follows:

$$l_{ij} = \sqrt{r_{ij}^2 + r_{ci}^2 - 2r_{ij}r_{ci}\cos(\theta_{ij} - \theta_{ci})}$$

$$\alpha_{ij} = \tan^{-1}\left(\frac{r_{ij}\sin(\theta_{ij}) - r_{ci}\sin(\theta_{ci})}{r_{ij}\cos(\theta_{ij}) - r_{ci}\cos(\theta_{ci})}\right) \quad (3.2)$$

where r_{ij} , r_{ci} , θ_{ij} , and θ_{ci} are the fuzzy numbers which represent the values of r_{ij} , r_{ci} , θ_{ij} , and θ_{ci} respectively.

3.1 Fuzzification

The fuzzification process must be carried out before any attempt to fuse fuzzy data. For given fuzzy numbers, r_{ij} , r_{ci} , θ_{ij} , and θ_{ci} , membership functions can have the different shapes depending on the attributes of feature points, F_{ij} and F_{ci} . For the sake of computational efficiency and ease of data acquisition, we represent the uncertainties of the measured data by use of a triangular fuzzy number. A triangular fuzzy number \tilde{m} denoted by (m, a, b) is defined as follows:

$$\tilde{m}(t) = \begin{cases} 1 - |m-t|/a, & \text{if } m-a \leq t \leq m \\ 1 - |m-t|/b, & \text{if } m \leq t \leq m+b \\ 0, & \text{otherwise} \end{cases} \quad (3.3)$$

where m is the center and positive numbers a and b are the left and right spread of \tilde{m} respectively.

We should determine the magnitudes of $|a-m|$ and $|b-m|$ in proportion to the uncertainties of the measured data. So for a given fuzzy number, \tilde{r}_{ij} , we determine the values m , a , and b by following rules:

Rule 1. $m = \tilde{r}_{ij}$.

Rule 2. $|a-m| = r_{ij}$.

Rule 3. $|b-m| = r_{ci}$, $w_{ci} = w_{ij}$.

Rule 4. $|a-m| = |b-m|$.

Similarly, for a given fuzzy number, $\tilde{\theta}_{ij}$, we determine the values m , a , and b by following rules:

Rule 1. $m = \tilde{\theta}_{ij}$.

Rule 2. $|a-m| = |b-m| = |g|$, $\frac{1}{w_{ci}} = \frac{1}{w_{ij}}$.

Fig. 6 shows the examples of fuzzy numbers, \tilde{r}_{ij} , r_{ci} , $\tilde{\theta}_{ij}$, and $\tilde{\theta}_{ci}$.

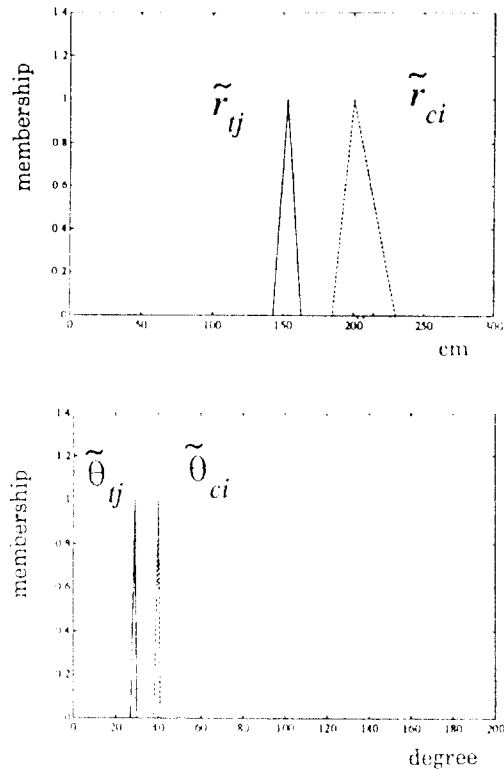


Fig. 6. Fuzzy numbers, r_{ij} , r_{ci} , θ_{ij} , and θ_{ci} for the feature points, F_{ij} and F_{ci} in Fig. 3 where $i = 6$ and $j = 4$.

3.2 Manipulation of Fuzzy Number Operation

We can operate (3.2) using fuzzy arithmetic[11]. The manipulation of fuzzy number operation can be processed by means of the extension principle of Zadeh[12]. This principle is one of the most basic concepts of fuzzy set theory which can be used to generalize crisp mathematical concepts to fuzzy sets. The extension principle allows us to induce from x fuzzy sets A_i a fuzzy set B on Y through f such that

$$\mu_B(y) = \begin{cases} \sup_{(x_1, \dots, x_n) \in f^{-1}(y)} \min(\mu_{A_1}(x_1), \dots, \mu_{A_n}(x_n)) & \text{if } f^{-1}(y) \neq \emptyset \\ 0 & \text{if } f^{-1}(y) = \emptyset \end{cases} \quad (3.4)$$

where $f^{-1}(y)$ is the inverse image of y , $\mu_{A_i}(y)$ is the greatest among the membership values $\mu_{A_1}, \dots, \mu_{A_n}$.

A (x_1, \dots, x_n) of the realization of y using x tuples

(x_1, \dots, x_r) .

It is not trivial to obtain a solution using (3.4) since a nonlinear programming problem must be resolved. However, fortunately, there is efficient and simple calculation based on the α -cut representation of fuzzy numbers and interval analysis[11]. Fig. 7 is results from the operation of fuzzy number in Fig. 6.

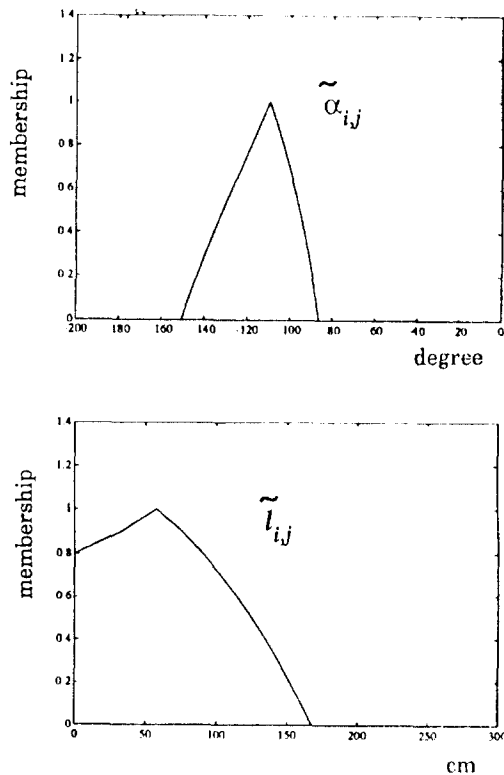


Fig. 7 Results from the operation of fuzzy number in Fig. 6.

3.3 Defuzzification

It is important to recover crisp data from the output fuzzy numbers. The fuzzy number is defuzzified to a crisp value within the universe of discourse of the output. With the widely used center of area(COA) strategy, we can directly compute the crisp value. The COAs, l_{ij} and α_{ij} of the fuzzy numbers, \tilde{l}_{ij} and $\tilde{\alpha}_{ij}$ are given by

$$l_{ij} = \frac{\sum_{k=1}^p (l_{ij})_k \cdot \mu_{\tilde{l}_{ij}}((l_{ij})_k)}{\sum_{k=1}^p \mu_{\tilde{l}_{ij}}((l_{ij})_k)}, \alpha_{ij} = \frac{\sum_{k=1}^q (\alpha_{ij})_k \cdot \mu_{\tilde{\alpha}_{ij}}((\alpha_{ij})_k)}{\sum_{k=1}^q \mu_{\tilde{\alpha}_{ij}}((\alpha_{ij})_k)} \quad (3.5)$$

where p, q are the numbers of quantization levels of the distance, l and the azimuth, α respectively. The defuzzified values l_{ij} and α_{ij} from \tilde{l}_{ij} and $\tilde{\alpha}_{ij}$ in Fig. 6 are 65 cm and 246° respectively.

3.4 Fusion of Defuzzified Values

Since a feature matching generates an output pair l_{ij}, α_{ij} , we should fuse the output pairs obtained from each feature matching using a proper scheme. In this paper, the weighted average method is introduced to fusion. We can infer the degree of reliability of the

output pair l_{ij}, α_{ij} using the attributes of the feature and the characteristics of the sensors. The final solutions are obtained by the following equations:

$$l_R = \frac{\sum_{(i,j)} K_{r(i,j)} \cdot K_{\theta(i,j)} \cdot l_{ij}}{\sum_{(i,j)} K_{r(i,j)} \cdot K_{\theta(i,j)}}, \alpha_R = \frac{\sum_{(i,j)} K_{r(i,j)} \cdot K_{\theta(i,j)} \cdot \alpha_{ij}}{\sum_{(i,j)} K_{r(i,j)} \cdot K_{\theta(i,j)}} \quad (3.6)$$

where (i, j) is the index pair of F_{ci} and F_{tj} matched successfully.

Note that the weights of (3.6) are determined as follows:

$$\begin{cases} K_{r(i,j)} = \frac{K_r'}{r_{ci} + r_{tj}}, \text{ for } r_{ci} + r_{tj} \geq K_r' \\ K_{r(i,j)} = 1, \text{ for } r_{ci} + r_{tj} < K_r' \end{cases} \quad (3.7)$$

$$\begin{cases} K_{\theta(i,j)} = \frac{|\theta_{ci} - \theta_{tj}| + K_\theta'}{K_{\theta''}}, \text{ for } |\theta_{ci} - \theta_{tj}| < K_\theta' \\ K_{\theta(i,j)} = 1, \text{ for } |\theta_{ci} - \theta_{tj}| > K_\theta' \end{cases} \quad (3.8)$$

where K_r' is determined by the precision of an ultrasonic sensor, K_θ' is the boundary value that increases the error in calculating (2.1), and $K_{\theta''}$ is the factor deciding the magnitude of $K_{\theta(i,j)}$.

(3.7) means that l_{ij} and α_{ij} have the lower reliabilities as $r_{ci} + r_{tj}$ increases because of the noise effect to the sensor. And (3.8) means that l_{ij} and α_{ij} have the higher reliabilities as $|\theta_{ci} - \theta_{tj}|$ increases because the more $|\theta_{ci} - \theta_{tj}|$, the better the matching feature point can represent the geometric relation.

IV. Experimental Results

To show the usefulness of the proposed environment model and fusion algorithm, a simple experiment is carried out. At first, we obtain the omnidirectional intensity and range data at the interval of 0.5° and 1° respectively at the target location and the current location by means of the scanner equipped with a CCD camera and an ultrasonic sensor. The height of the horizontal plane is 1.2m. The intensity value of each horizontal direction is the average of intensity values lying vertically within the range of 5° in the center of the horizontal plane. The geometric relation between the current location and the target location is $l = 67\text{cm}$ and $\alpha = 244^\circ$. Fig. 8 is the photograph of the scanner. Fig. 9 is the panoramic image obtained at the target location and the current location. The intensity data of the middle horizontal line in Fig. 9 are represented in Fig. 3. The index pairs of finally matched feature points, F_{ci} and F_{tj} are (6, 4), (9, 8), (23, 23), and (25, 25). Table 1 shows the results obtained from each matched point in three cases of using measured values, fuzzy singletons, and fuzzy sets. And the final solutions are obtained by (3.6) in each case, where $K_r' = 300\text{ cm}$, $K_\theta' = 20^\circ$, and $K_{\theta''} = 40^\circ$. From the results, we can verify that in the case of using fuzzy number the final solutions have the less errors than those obtained from measured values. It can also be seen that the final solutions have the less errors in the case of using fuzzy set than in

that case of using fuzzy singleton.

Table 1. Results obtained from each matched feature point.

Index pair (i, j)	Case of using the measured value		Case of using the fuzzy singleton		Case of using the fuzzy set	
	$l_{i,j}$ (error) unit:cm	$a_{i,j}$ (error)	$l_{i,j}$ (error) unit:cm	$a_{i,j}$ (error)	$l_{i,j}$ (error) unit:cm	$a_{i,j}$ (error)
(6, 4)	52 (15)	252° (7°)	58 (9)	250° (6°)	65 (1)	245° (1°)
(9, 8)	146 (-79)	254° (10°)	146 (-79)	254° (10°)	145 (-78)	254° (10°)
(23, 23)	53 (14)	225° (11°)	58 (8)	254° (10°)	59 (8)	249° (-5°)
(25, 25)	22 (45)	217° (-27°)	19 (48)	205° (-39°)	50 (17)	213° (-31°)
Final solution	58 (9)	249° (5°)	62 (5)	246° (2°)	68 (-1)	243° (-1°)

V. Conclusion

We have proposed a new environment model for local homing for the indoor mobile robot using the

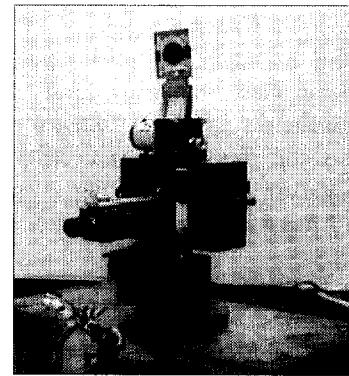


Fig. 8. Photograph of the scanner.

omnidirectional sensor data. And we have developed a sensor fusion method that can deal with the sensor data including uncertainty. The proposed method uses fuzzy numbers in order to represent the subjective knowledge and manipulates the operation of uncertain quantities using fuzzy arithmetic. As you observed in the experiment results, the proposed model and method are effective to the indoor mobile robot navigation.

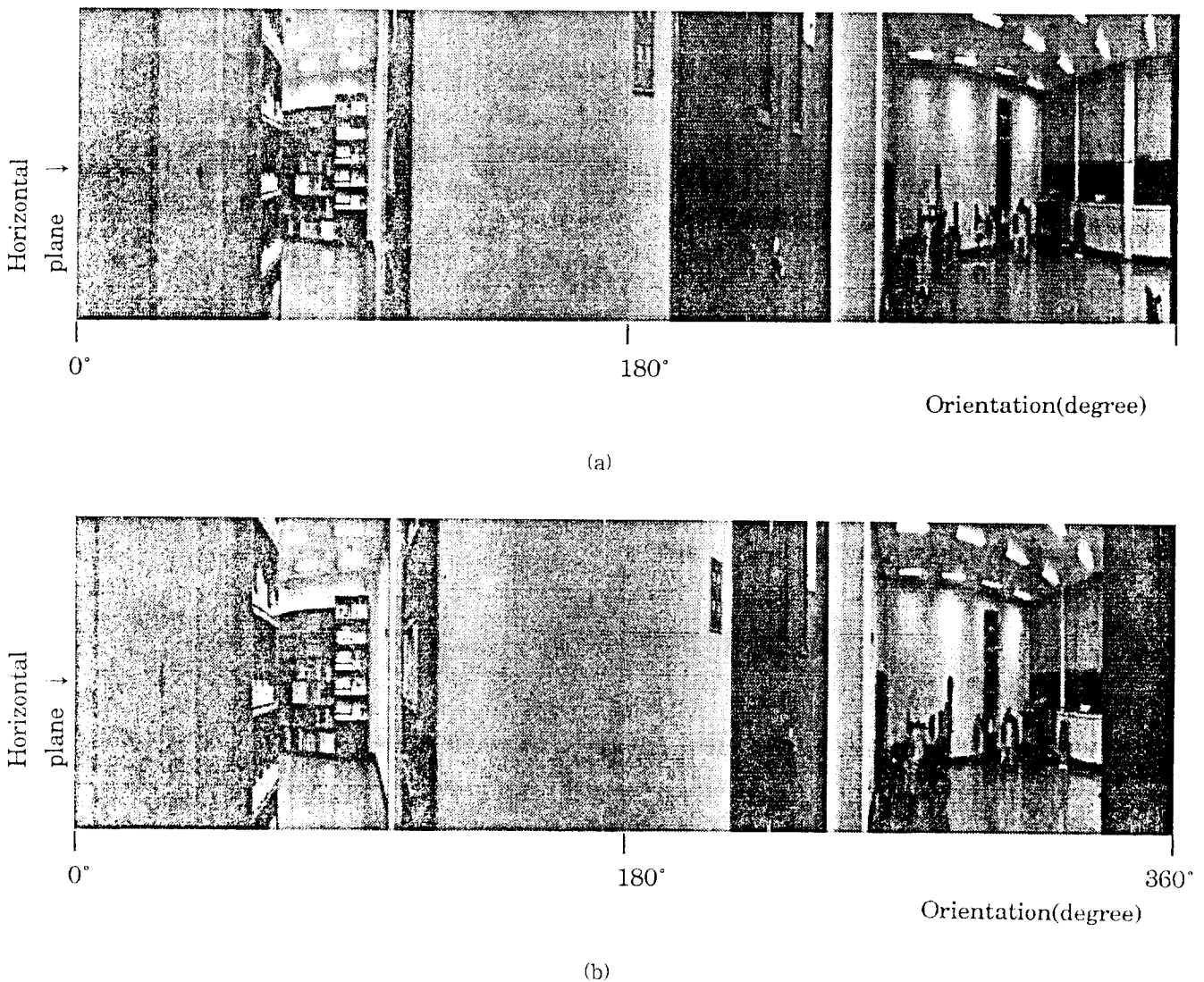


Fig. 9. Panoramic image, (a) Image obtained at the target location, (b) Image obtained at the current location.

Reference

- [1] C. Fennema, A. Hanson, E. Riseman, J. R. Beveridge, and R. Kumar, "Model-Directed Mobile Robot Navigation," *IEEE Trans. System, Man, and Cybernetics*, vol. 20, no. 6, pp. 1352-1369, Nov./Dec. 1990.
- [2] N. Ayache and O. D. Faugeras, "Maintaining Representations of the Environment of a Mobile Robot," *IEEE Trans. Robotics and Automation*, vol. 5, no. 6, pp. 804-819, Dec. 1989.
- [3] G. Adiv, "Determining Three-Dimensional Motion and Structure from Optical Flow Generated by Several Moving Objects," *IEEE Trans. Pattern Anal. Mach. Intell.*, vol. 7, no. 4, pp. 384-401, July 1985.
- [4] J. Y. Zheng and S. Tsuji, "Panoramic representations of scenes for route understanding", *Proc. Tenth Int. Conf. Pattern Recognition*. IEEE Computer Soc. Press. pp. 161-167, 1990.
- [5] J. Hong, X. Tan, B. Pinette, R. Weiss, and E. M. Riseman, "Image-based Homing," *Proc. IEEE Conf. Intelligent Robots and Systems*, pp. 620-625, 1991.
- [6] C. Ferrell, "Many Sensors, One Robot," *Proc. IEEE Conf. Intelligent Robots and Systems*, pp. 399-406, July 1993.
- [7] M. Abdulghafour, T. Chandra, and M. A. Abidi, "Data Fusion Through Fuzzy Logic Applied to Feature Extraction From Multi-Sensory Images," *Proc. IEEE Conf. Intelligent Robots and Systems*, pp. 359-366, 1993.
- [8] H. F. Durrant-Whyte, *Integration, Coordination, and Control of Multi-Sensor Robot System*, Kluwer Academic Pub., Boston, 1987.
- [9] C. R. Smith, "A Bayesian approach to multisensor data fusion," *Proc. SPIE*, vol. 1699, pp. 285-299, 1992.
- [10] W. J. Kim, J. H. Ko and M. J. Chung, "Uncertain robot environment modelling using fuzzy numbers," *Fuzzy sets and systems*, 61, pp. 53-62, 1994.
- [11] A. Kaufman and M. M. Gupta, *Introduction to Fuzzy Arithmetic*, Van Nostrand Reinhold, New York, 1985.
- [12] L. A. Zadeh, "The concept of a linguistic variable and its application to approximate reasoning-I", *Information Science* 8, pp. 199-249, 1975.
- [13] W. K. Pratt, *Digital Image Processing*, Second Edition, Wiley-Interscience, New York, pp. 497-517, 1991.



방석원

1964년 4월 19일생. 1988년 서울대학교 공과대학 전기공학과 졸업. 1991년 한국과학기술원 전기 및 전자공학과 졸업(공학 석사). 현재 동 대학원 전기 및 전자공학과 박사과정 재학중.

정명진

1950년 1월 31일생. 1973년 서울대학교 공과대학 전기공학과 졸업. 1977년 미국 미시간 대학교 ECE 졸업. 1983년 동 대학원 CICE 졸업(공학 박사). 1976년 국방과학연구소 연구원. 1981~1983년 미시간 대학교 CRIM 연구조교. 1983년 ~ 현재 한국과학기술원 전기 및 전자공학과 교수.